Biochar enhanced the nitrogen removal performance of heterotrophic nitrification-aerobic denitrification strain *pseudomonas fluorescent* sp. Z03 for insufficient carbon source wastewater under low temperature

Jie Jiang (xuxiaoyan11232@163.com)
Qufu Normal University
XiaoyanXu (344637803@qq.com)
Qufu Normal University
Zhina Guo (1610180996@qq.com)
Qufu Normal University
Lianglun Sun (xiaoyanxu11232@outlook.com)
Qufu Normal University
Meizhen Tang (xuxiaoyan3112@163.com)
Qufu Normal University

Research Article

Keywords: heterotrophic nitrification-aerobic denitrification, biochar, nitrogen removal, low-temperature

Posted Date: October 8th, 2021

DOI: https://doi.org/10.21203/rs.3.rs-916848/v1

Abstract

In this study, biochar BC400 and BC700 were prepared, characterized and coupled with heterotrophic nitrification-aerobic denitrification (HNAD) strain Z03 for nitrogen removal experiments. The characterization results showed that BC700 has a higher specific surface area and a more complex multilayered pore structure, with increased aromatic condensation and higher crystallinity. BC400 and BC700 both have good redox activity, while BC400 has stronger electron donor capacities and BC700 owns better electron transfer properties. In addition, both BC400 and BC700 contain relatively high levels of dissolved organic carbon (DOC), reaching at 62.95 and 51.617mg/g respectively. BC400/BC700 coupled with strain Z03 can significantly improve the NH_4^+-N removal performance of low-temperature and low C/N wastewater compared with the control group. At a dosage of 4.0 g/L, the removal rate of NH_4^+-N reached to 95.16% (BC400 + Z03) and 84.37% (BC700 + Z03) within 72h, respectively. Higher than the sum of adsorption by BC400/BC700 (16.19%/18.85%) and microbial degradation (41.03%). Besides, the BC400 + BC700 + Z03 NH_4^+-N removal systems provide higher nitrogen removal efficiencies than BC400/BC700 + Z03 nitrogen removal systems. When the dosage (BC400 + BC700, mass ratio 5:1) reaches 3.0g/L, it can achieve more than 90% NH_4^+-N removal rate within 48h. The reasons for the promotion of biochar on microbial denitrification were analyzed as follows: 1) DOC can provide an additional carbon source for microorganisms; 2) biochar, as a pH buffer, can neutralize the acidity due to nitrification; 3) BC400 and BC700, as materials with good redox activity, may play a role in promoting the activity of electron transfer system and enzyme activity.

1. Introduction

Nitrogen pollution in China’s water bodies has been a long-standing problem, and human activities have fundamentally altered the nitrogen cycle (Galloway et al., 2008).The current situation of nitrogen pollution in China is directly related to the rapid development of agriculture and various manufacturing industries. China's current nitrogen fertilizer consumption accounts for about 32% of the world's total nitrogen fertilizer consumption, and the massive use of nitrogen fertilizer and unreasonable irrigation methods result in urea, NH_4^+-N and NO_3^--N entering surface water bodies through surface runoff and other means. In addition, livestock waste water, domestic sewage and industrial wastewater are also the main sources of nitrogen in water bodies (Liu and Wang, 2019). Agricultural systems in China account for 59% of current surface water nitrogen emissions, while the other 39% comes mainly from domestic waste (13% from urban sewage, 8% from rural sewage and 18% from organic waste) and the remaining 2% from industrial waste. Excessive nitrogen content in water bodies is one of the main causes of eutrophication and marine red tides, and the nitrite accumulated during the nitrogen cycle is toxic and carcinogenic to humans. (Liu and Wang, 2019; C. Q. Yu et al., 2019), Nitrogen pollution in water bodies also increases the risk of methemoglobinemia (Huang et al., 2012), bladder cancer and lung cancer in humans (C. Wang et al., 2019). The studies (C. Q. Yu et al., 2019; Zhang et al., 2015) points out that if the total nitrogen concentration in the effluent of domestic wastewater treatment plants in China is reduced from 15mg/L to 5mg/L, the nitrogen discharge from water bodies can be reduced by 5%-10%.

Although the research on biological denitrification has gradually become systematic, many urban domestic sewage treatment plants still have difficulties in meeting the increasingly stringent effluent standards due to the interference of various problems in practical application. Microbial degradation is often limited in practice by slow cell growth, stimulation of substrate concentration and environmental conditions (Chen et al., 2016; Gao et al., 2011; Yuan et al., 2011). Both practical results and existing studies have shown that low C/N and low temperature conditions can significantly inhibit the biological nitrogen removal effect (Chen et al., 2019; Li et al., 2015; C. Wang et al., 2019). Under the strategy of "energy saving and emission reduction", the concentration of organic matter in the influent water of urban sewage treatment plants is gradually reduced, and the problem of insufficient organic carbon sources available for microorganisms is often faced in the process of nitrogen removal. The electron donor is the rate-limiting substrate that controls substrate utilization and biological growth kinetics. Denitrification process is inhibited under the condition of low C/N, which easily leads to the production of carcinogenic nitrite and affects the total nitrogen concentration in the effluent. Survey data shows that currently 10% of China's wastewater treatment plants require additional carbon sources to meet the demand for denitrification, and about 50% of urban wastewater treatment plants in southern areas with high rainfall, such as the Taihu Lake basin (Jie and He, 2018). Organic electron donor is the most commonly exogenous electron donor in denitrification process. However, the effect of electron donor dosing is easily affected by the fluctuation of influent volume and water quality, and the unsuitable dosing is likely to lead to the increase of sludge and nitrate accumulation, so the selection of carbon source type and accurate dosing is one of the main problems facing biological denitrification at present.

Biochar is a stable carbon-rich by-product synthesized by pyrolysis and carbonization of primary biomass of plants and animals, which is itself an environmentally friendly material for reuse of waste resources. Its practical applications include carbon sequestration, soil fertility improvement and pollution remediation, etc. (Ahmad et al., 2014a). With the increasing research on biochar, the role of biochar in the field of pollutant removal has changed from traditional adsorbent to diversified occurrence, such as being a microbial immobilization carrier (Tang et al., 2020; Yang et al., 2020), fertilizer slow release carrier (Li et al., 2020) and electron doner(X. Xu et al., 2019). As a carbon rich material with low toxicity and high porosity, biochar can promote microbial film growth, enhance microbial adaptation to the environment and provide carbon sources in practical applications (Sima et al., 2017), which can effectively promote biological denitrification in combination with microbial immobilization and coupled material dosing (Lou et al., 2019). In addition, biochar has a variety of functional groups, and the resulting redox properties enable it to participate in redox reactions in the environment in different ways, thus accelerating its removal of pollutants. Previous studies have shown that differences in carbonized temperatures lead to different pore structures and redox properties of biochar, which in turn lead to different adsorption degradation and mediating mechanisms in the removal of pollutants(X. Xu et al., 2019; Z. Xu et al., 2019). In the redox system, the electron donor capacity and electron-mediated ability of biochar can promote the electron transfer and enzymatic activity of the system, thus enhancing the biological denitrification(Wu et al., 2019a). However, there are few studies on the coupling of biochar with microbial denitrification at

different carbonized temperatures, thus the promotion mechanism of biochar in biological denitrification process should be investigated in depth.

With these considerations, the aims of this study were thus to: (1) analysis the physicochemical properties of chestnut shell biochar at different carbonization temperatures,(2) investigate the effect of biochar coupled HNAD strain Z03 on the treatment of low C/N wastewater(3) explore the mechanism of biochar-enhanced microbial ammonia nitrogen removal efficiency.

2. Materials And Methods

2.1 Materials source

The HNAD strain *pseudomonas fluorescent* sp. Z03 was isolated from piggery sewage treatment system in Qufu city, Shandong province, China. The chestnut shells were washed repeatedly with distilled water, drained and dried, crushed and ground, and then passed through a 100-mesh nylon sieve to get the powder.

2.2 Preparation and characterization of biochar

The biochar was prepared by oxygen-limited and temperature-controlled carbonization method. An appropriate amount of chestnut shell powder was taken in a porcelain boat and placed in a vacuum tube furnace. After the vacuum pump was pumped to negative pressure, the vacuum tube furnace was heated to 400 ℃ and 700 ℃ at a rate of 10 ℃/min, and then the tube furnace was closed after 1 h of carboning time. The biochar yield was about 32%.

The experiments were carried out to analyze the elemental composition of the prepared BC400 and BC700 by elemental analyzer. The specific surface area sizes of BC400 and BC700 were determined by specific surface area analyzer (BET). The shape, surface morphology and material dimensions of BC400 and BC700 were characterized by thermal field emission scanning electron microscopy (SEM). The infrared absorption spectra of BC400 and BC700 were obtained by Fourier transform infrared spectroscopy (FTIR) in the spectral range of 400 to 4000 cm^{-1}. The characteristic wave numbers of specific bands of the spectra were analyzed to obtain the species of the main functional groups on the surface of the materials to infer the NH4+-N removal mechanism. The zeta potentials of the materials were measured at different pH values to obtain the zero sites, which provide a basis for the study of the adsorption properties and the direction of material modification. The structural characteristics and graphitization degree of the synthesized materials were characterized by Raman spectroscopy (RS) to investigate the electrical conductivity of the materials. Analyze the structural changes and crystalline phase structure of the materials by X-Ray diffractomer (XRD). DOC contained in biochar was determined by total organic carbon (TOC) analyzer with reference to sequencing extraction method(Sima et al., 2017).

2.3 Configuration of wastewater

The purpose of this study is to investigate the nitrogen removal performance of low C/N wastewater under low temperature conditions. Combined with the actual pollutant concentrations of urban domestic wastewater and industrial wastewater, the initial COD of this experiment is 250 mg/L, the initial NH_4^+ concentration is 50 mg/L, and the initial TP is 2.5 mg/L of artificially simulate and domestic wastewater.

2.4 Batch experiments

To investigate the nitrogen removal effect of different biochar coupled strain Z03, the effects of BC400 / BC700 dosage (0.5–4.0 g/L), BC400 and BC700 mixing ratio (1:1–5:1) and BC400 + BC700 at different pH (5.5–10.5) on the nitrogen removal effect of strain Z03 were investigated. Except for the pH experiments, each group was set up in three parallel in 250mL conical flasks with 95mL of nitrogenous wastewater at an initial pH of 7.0 and 5mL of Z03 bacterial solution. At the same time, a control group with only the corresponding amount of biochar and Z03 bacterial solution was set up in each group. The above mixed solution was incubated at 120rpm in a full temperature shaker at 10℃, and the OD600 value of the bacterial solution was measured at 12h, 24h, 36h, 48h, 60h and 72h. The content of ammonia nitrogen, nitrate nitrogen and nitrite nitrogen in the sample was measured by passing the water sample through 0.45μm filter membrane with a syringe, and the pH value of the water sample was also measured.

2.5 Analytical Methods

PH was measured by pH meter (HQ11d, HACH). The OD_{600} of the isolate was measured by a double beam spectrophotometer (UV-T9, Puxi, Beijing) at 600 nm. Besides, culture samples filtered by passing the sample through a 0.45 μm filter for chemical analysis. The ammonium concentration was determined by the Nessler's reagent spectrophotometry method, nitrate concentration was determined by the method of phenol disulfonic acid photometry and nitrite concentration was measured according to N-(1-naphthalene)-diaminnoethane photometry method.

3. Results And Discussion

3.1 Biochar characterization

The SEM images and physicochemical properties of BC400 and BC700 are shown in Fig. S1 and Table 1, respectively. Biochar is a carbon rich material with pore size structure and its properties are related to the carbonization temperature(Ahmad et al., 2014b; Guerrero et al., 2008). During the pyrolysis process, the elemental C content of biochar increased with the increasing carbonization temperature. Previous study showed that the DOC content of biochar prepared from different biomasses varies greatly, and the DOC content of biochar decreases as the carbonization temperature increases(Liu et al., 2019). BC400 and BC700 contained relatively high DOC contents of 62.95 and 51.617 mg/g, respectively. The pH_{pzc} of BC400 was 3.1 and that of BC700 was 4.3 obtained by zeta potential test (Fig.S2), which may be due to the fact that BC400 contains more oxygenated acidic functional groups (Y. Yu et al., 2019). The pH_{pzc} of

both BC400 and BC700 were lower than 4.5, indicating that the biochar was negatively charged in the experimental pH range (5.5–9.5) and could produce electrostatic adsorption of cations.

Table 1
Physicochemical properties of BC400 and BC700

Biochar	C(%)	H(%)	N(%)	DOCmg/g	pH_{pzc}	Multi-point BET specific surface area(m^2/g)	Single-point total pore volume (cc/g)	Single-point average pore radius (nm)
BC400	64.16	3.68	1.42	62.95	3.1	3.0407	0.034266	22.54
BC700	76.85	1.79	1.34	51.61	4.3	155.096	0.085977	1.11

Both BC400 and BC700 have obvious multi-stage pore structure and the pore size type is mainly microporous, but BC700 has significantly more pore size structure and the specific surface area reaches 155.096 m^2/g. The nitrogen adsorption-desorption isotherms and pore size distributions of BC400 and BC700 are shown in Fig. 1a and Fig. 1b. The adsorption-desorption isotherms of BC400 and BC700 were type III and type I, respectively. The adsorption capacity of BC400 increases gradually with the increase of the partial pressure of nitrogen (P/P_0), and there is no obvious hysteresis loop in the curve, which indicates that it contains multi-level pore structure, but the number of pore size is small. The adsorption saturation of BC700 was basically reached in the low-pressure region, indicating that it contains a large number of micropores (< 2 nm). The adsorption amount increased slightly at P/P_0 of 0.4–0.8 and there was an H4-type hysteresis loop, indicating the presence of mesopores (2 ~ 50 nm). The rich pore size structure and high specific surface area of biochar provide the feasibility of adsorption and carrier.

The FTIR results of BC400 and BC700 are shown in Fig. 1c. It can be seen that BC400 and BC700 contain various types of functional groups, such as hydroxyl group (-OH, 3440 ~ 3340 cm^{-1}), aliphatic C-H bond (2960 ~ 2890 cm^{-1}), benzene ring skeleton vibration C = C (1650 ~ 1450 cm^{-1}), carboxyl group (-COOH, 720 cm^{-1} and 1380 cm^{-1}), etc. The series of absorption peaks of C = O from 1850 to 1650 cm^{-1} indicated the presence of ketone and quinone groups, and the stretching vibration of C-O and the presence of OH bonds indicated the presence of alcohol and phenol groups (S. Wang et al., 2019). FTIR analysis showed that BC400 contains more oxygen-containing functional groups, which indicated that it has the potential to participate in redox reactions (X. Xu et al., 2019); BC700 contains more conjugated π-structures, which allows electron transfer through the off-domain formed by the hybridization of large π-bond orbitals on thick benzene, thus providing better electron transfer performance (Klüpfel et al., 2014; Wu et al., 2019a; Z. Xu et al., 2019).

In order to investigate the structural changes and crystal composition of biochar at different carbonization temperatures, XRD analysis (Fig. 1d) was performed on BC400 and BC700, respectively.

Results showed two broad and slow amorphous diffraction peaks at 2θ of 24° and 43°, which are graphite microcrystalline d_{002} and d_{101} diffraction peaks, respectively (Wang et al., 2016). Since the biochar used in the experiment was treated with water washing and almost free of salts, no obvious sharp diffraction peaks were seen. The XRD pattern shows that as the carbonized temperature increases, the peak intensity of BC700 increases compared to BC400, the peak area increases, and the crystallinity increases.

Raman spectroscopy is an effective means to characterize the bond structure of carbon nanomaterials. the characteristic peaks located at about 1350 cm^{-1} and 1530 cm^{-1} in the Raman spectrum correspond to the D and G peaks of the material, which characterize the lattice defects and graphitization of carbon atoms, respectively. The intensity ratio of the D and G peaks, i.e., the value of I_D/I_G, reflects the degree of defects and graphitization of the carbon nanomaterials structure, and the value is related to The ratio of sp^3 hybridized carbon to sp^2 hybridized carbon (Sima et al., 2017). From the Raman spectrograms of BC400 and BC700 (Fig. 1e and Fig. 1f), it can be seen that the I_D/I_G of BC400 (2.51) is higher than that of BC700 (1.59), which indicated that as the carbonized temperature increases, the graphitization of the material increases, the structural defects decrease, and the overall structure becomes more ordered. Feng et al. (Feng et al., 2002) found that the basic units of biochar structure were randomly oriented at temperatures below 700°C, but in the temperature range of 700 to 1500°C they were rearranged and structural defects were removed, resulting in a more ordered structure of the carbonaceous solids. Marsh (Marsh, 1987) found that during biomass heating, the decomposition of ether-type groups led to a decrease in the distance between aromatic layers, and thus the structure of biochar at higher carbonized temperatures became more ordered.

Figure 1 Nitrogen adsorption-desorption isotherms of BC400 and BC700 (a); pore size distribution of BC400 and BC700(b); FTIR spectrograms of BC400 and BC700(c); XRD spectrograms of BC400 and BC700 (d); Raman spectrograms of BC400 (e) and BC700 (f).

3.2 Effect of BC400/BC700 on HNAD process

3.2.1 Effect of BC400/BC700 dosage

The changes of NH_4^+-N concentration, pH, NO_3^--N and NO_2^--N concentration of BC400/BC700 + Z03 system with different biochar dosages are shown in Fig. 2a and Fig. 2b. The removal effect of NH_4^+-N in both BC400 + Z03 and BC700 + Z03 systems increased with the increase of biochar dosage and reached the best NH_4^+-N removal efficiency at the dosage of 4.0 g/L. When the dosage was greater than 3.0g/L, the concentration of NH_4^+-N in both systems could be reduced to less than 10mg/L within 72h, but the NH_4^+-N removal efficiency of BC400 + Z03 system was slightly better than that of BC700 + Z03 system, and when the dosage was 4.0g/L, the concentration of ammonia nitrogen in both systems could be reduced to 2.42mg/L and 7.81mg/L respectively. In the BC700 + Z03 system, when the BC700 dosage was lower than 3.0 g/L, the NH_4^+-N concentration in each group showed a small rebound from 12 h to 24

h, and then decreased steadily. The adsorption experiments results (Fig.S3) showed that the biochar reached the saturation of ammonia nitrogen adsorption within 12 h, and the NH_4^+-N concentration rebounded with the increase of reaction time, and the ammonia nitrogen desorption, so it was speculated that this phenomenon might be related to the adsorption desorption of biochar. In addition, there was no significant accumulation of intermediate products in both systems throughout the NH_4^+-N removal process, and the concentrations of NO_3^--N and NO_2^--N were stable below 1.0 mg/L and 0.15 mg/L, respectively. The pH of BC400 + Z03 system decreased continuously, and finally stabilized at about 4.25. In BC700 + Z03 system, when the BC700 dosage was lower than 1.0g/L, the pH decreased continuously, and when the dosage was 2.0 ~ 4.0g/L, the pH increased within 12h, decreased continuously within 12 ~ 48h, but increased again after 48 ~ 72h. The final pH of each group ranged from 4.0 to 7.5 with the dosage from low to high.

In order to compare the NH_4^+-N removal efficiency of the BC400/BC700 + Z03 system with the control group, the NH_4^+-N removal efficiency and the corresponding pH of each system at 72 h of reaction are shown in Fig. 2c. Strain Z03 inoculated with 5% inoculum to artificial wastewater could achieve 41.03% NH_4^+-N removal efficiency at 72h, which was higher than the efficiency of biochar adsorption at each dosage, but significantly lower than that of biochar coupled with strain Z03. In addition, the removal effect of biochar on NH_4^+-N was not significantly correlated with the dosage, and the maximum NH_4^+-N removal efficiency was 31.96% at the dosage of 0.5 g/L for BC400 and 26.60% at the dosage of 2.0 g/L for BC700. The adsorption was the main method. The pH was significantly different among the systems after 72 h, and the difference between the groups within the same system was not significant. The higher the NH_4^+-N removal efficiency of the system, the lower the pH value at 72 h. The final pH of BC400 + Z03, Z03 and biochar NH_4^+-N removal systems were around 4.5, 6.0 and 7.5, respectively, but the pH of BC700 + Z03 system increased with the increase of the dosage.

Figure 2 Variation of NH_4^+-N concentration, pH, NO_3^--N and NO_2^--N concentration in BC400 + Z03 (a) and BC700 + Z03 (b) systems with different biochar dosages; comparison of NH_4^+-N removal efficiency and pH between BC400/BC700 + Z03 systems and control group at different biochar dosages for 72h (c).

In order to further investigate the difference of the NH_4^+-N removal efficiency between BC400 and BC700 coupled strain Z03, the experiments compared the ammonia nitrogen removal rate and pH of three systems, BC400 + Z03, BC700 + Z03 and strain Z03, at 72h of reaction, and the results are shown in Fig. 3. It can be seen that the NH_4^+-N removal efficiency of biochar coupled strain Z03 NH_4^+-N removal system was higher than that of strain Z03 NH_4^+-N removal system under each dosage, and the NH_4^+-N removal efficiency increased with the increasing dosage. When the dosage was 0.5 g/L, the NH_4^+-N removal efficiency of BC400 + Z03, BC700 + Z03 and Z03 systems were 47.05%, 43.83% and 41.04%, respectively. When the dosage was 1.0 g/L and 2.0 g/L, the NH_4^+-N removal efficiency of BC700 + Z03 system was higher than the other two systems, and the NH_4^+-N removal efficiency could reach 72.02%. When the

dosage was 3.0 g/L and 4.0 g/L, the NH_4^+-N removal efficiency of BC400 + Z03 system was significantly higher than the other two systems, reaching 89.74% and 95.16%, respectively, while the NH_4^+-N removal efficiency of BC700 + Z03 system was 82.91% and 84.37%, respectively.

Biochar, as a carbon-rich material with a multilayer pore structure, can slowly release DOC to provide an additional carbon source for strain Z03. The measurement results of DOC contained in BC400 and BC700 showed that BC400 and BC700 contained relatively high DOC content, 62.95 and 51.617 mg/g, respectively, which may be related to the biomass material and the carbonization temperature. It has been shown that biochar can release bioavailable soluble organic carbon and promote denitrification reactions (Mukherjee and Zimmerman, 2013; Sima et al., 2017; Steinbeiss et al., 2009). Tang et al. (Tang et al., 2016)characterized soluble organic matter in birch and maple biochar by optical analysis and found that carbonization temperature can affect the composition of soluble organic matter in biochar, which in turn affects the bioavailability of dissolved organic matter. This is probably the main reason why the NH_4^+-N removal efficiency of the BC400 + Z03 system is better than that of BC700 + Z03 at high dosing rates, while the adsorption effect of biochar at low dosing rates plays a major role in the NH_4^+-N removal process.

The experimental results revealed that biochar has a pH retarding effect, which can neutralize the acidity due to nitrification reaction and reduce the inhibitory effect of water pH on enzyme activity. The nitrification and denitrification processes are highly susceptible to the influence of environmental pH. Nitrification is an acid-producing process, while denitrification is an alkaline-producing process. Microorganisms are extremely sensitive to the environmental pH, and either too high or too low pH will affect the biological denitrification effect (Ren et al., 2014; Zhang et al., 2012).

It is known that in the denitrification system with only strain Z03, the pH eventually decreased to about 6.0 as the reaction proceeded, and the nitrification rate of nitrifying bacteria usually slowed down significantly at pH below 6.5, which is another limiting factor for its denitrification effect in addition to the carbon source. In contrast, the pH of all groups with biochar only increased, indicating the presence of alkali in the biochar, which is the same as the previous study by Yuan et al. (Yuan et al., 2011). They studied the morphology of alkali presence in biochar using FTIR, XRD and potentiometric titration, and found that the release of alkali from biochar in the water column could be the effect of organic functional groups such as -COO- and -O- on its surface and the presence of carbonate in biochar, and the content of alkali in biomass char due to carbonate increased with the increase of carbonized temperature, while the effect of organic functional groups on alkali in biomass char was the same as On the contrary, this conclusion is consistent with the results of the present experiment in which the final pH of the groups in which BC700 was injected under the same conditions was higher than that of the BC400 group. In addition, in the BC400/BC700 + Z03 system, it can be seen that some groups showed a small increase and then decrease in pH within 12 h from the beginning of the reaction, which is due to the fact that strain Z03 is in the adaptation period to the environment, the nitrification reaction rate is low, and the alkaline material released from biochar makes the pH rise back, and then the pH of the system continues to

decrease as the reaction proceeds. After 48 h or 60 h, the rate of denitrification gradually decreased, and with the decrease of the reaction rate, the pH of each group with higher biochar dosage increased significantly, presumably because the concentration of ammonia and nitrogen in the system was too low, and the concentration of nitrification substrate and carbon source limited the reaction, but the biochar still continued to release alkaline substances, so the pH kept increasing. Therefore, biochar can be used as a pH buffer to neutralize the acidity generated by the nitrification process and continuously release alkaline components throughout the reaction to prevent the inhibitory effect on biological denitrification due to low pH. In addition, the variation of pH causes the variation of the adsorption capacity of biochar for ammonia nitrogen, which may be the reason why the adsorption effect of each system material was not significantly correlated with the dosage, and some groups obtained the highest adsorption effect at the lowest dosage.

Figure 3 Comparison of 72h NH_4^+-N removal rate and pH change between BC400/BC700 + Z03 and strain Z03 systems with different biochar dosages

3.2.2 Effect of BC400 + BC700 on HNAD process

Different carbonized temperatures of biochar have different physicochemical properties, and thus have various promotion mechanisms for microbial denitrification. In order to investigate whether the BC400 + BC700 + Z03 system has different NH_4^+-N removal effect than the BC400/BC700 + Z03 systems, this study designed the BC400 + BC700 coupled Z03 system and investigated the effects of dosage, mixing ratio and pH on the NH_4^+-N removal effect. The changes of NH_4^+-N concentration, pH, NO_3^--N and NO_2^--N concentration of BC400 + BC700 + Z03 system with different biochar dosages mixed at 1:1 mass ratio are shown in Fig. 4a. It can be seen that the NH_4^+-N removal efficiency of the BC400 + BC700 + Z03 system increased with the increase of the biochar dosing amount in 72 h. The NH_4^+-N concentration could be reduced to below 10 mg/L within 48 h when the dosage was 3.0 g/L and 4.0 g/L, and there was almost no accumulation of NO_3^--N and NO_2^--N. The pH of the system showed an overall decreasing trend within 72 h. The pH of the group with the dosing amount over 3.0 g/L increased after 48 h, and finally the pH of each system was in the range of 3.75 ~ 5.0 according to the dosing amount from low to high, respectively.

In order to compare the difference of NH_4^+-N removal efficiency between the BC400 + BC700 + Z03 system and the control group (only BC400 + BC700/strain Z03), the NH_4^+-N removal efficiency of each system at 72 h was compared in Fig. 4b. The results showed that the NH_4^+-N removal efficiency of BC400 + BC700 + Z03 system was significantly better than that of the control groups, and the highest NH_4^+-N removal efficiency was 94.36% when the mixed biochar dosage was 3.0 g/L. The efficiency of BC400 + BC700 adsorption was significantly lower than that of strain Z03 HNAD efficiency, and the NH_4^+-N removal efficiency were 25.74%, 24.12%, 27.49%, 15.66% and 16.61% for the mixed biochar dosage from 0.5 to 4.0 g/L, respectively. After 72 h of reaction, the final pH of the system with higher NH_4^+-N removal efficiency was lower. The final pH of each group with different dosage of BC400 + BC700 did not differ much and

was stable at 7.5 ± 0.2. The final pH of BC400 + BC700 + Z03 system gradually increased from 4.0 to 5.0 with the increase of dosage.

The above results showed that compared to the BC400/BC700 + Z03 system, the BC400 + BC700 + Z03 system was able to reduce the ammonia nitrogen concentration to less than 10 mg/L in a shorter reaction time when the biochar dosage exceeded 3.0 g/L. Figure 4c shows the changes in NH_4^+-N removal efficiency and pH of the BC400/BC700 + Z03 system and the BC400 + BC700 + Z03 systems at 48h and 72h, respectively. As can be seen from Fig. 4c, the NH_4^+-N removal efficiency of the BC400 + BC700 + Z03 system was significantly higher than that of the BC400/BC700 + Z03 system in the reaction 48 h at the dosing amounts of 3.0 g/L and 4.0 g/L, which could reach 87.36% and 86.56%, respectively. The mixed biochar system can significantly shorten the reaction time under the condition that the effluent ammonia nitrogen meets the standard. The differences in pH values between groups within each system were not significant. With the increase of reaction time to 72 h, the difference of NH_4^+-N removal efficiency of each system decreased, and the pH values of BC400 + BC700 + Z03 and BC700 + Z03 systems increased with the increase of biochar dosage. At the dosing of BC400 + BC700 only, the NH_4^+-N removal efficiency of all groups was lower than 30% at different dosing amounts, and the adsorption effect increased with the increase of initial pH.

Figure 4 Variation of NH_4^+-N concentration, pH, NO_3^--N and NO_2^--N concentration in BC400 + BC700 + Z03 system with different biochar dosages (a); comparison of NH_4^+-N removal efficiency and pH between BC400 + BC700 + Z03 systems and control group at different biochar dosages for 72h (b); comparison of NH_4^+-N removal efficiency and pH between BC400 + BC700 + Z03 and BC400 BC400/BC700 + Z03 systems with different biochar dosages(c).

Figure 5a shows the effect of the mixing ratio of BC400 and BC700, showing that when the dosage was 3.0 g/L and the mass ratios of BC400 and BC700 were 1:1, 2:1, 3:1, 4:1 and 5:1, respectively, all groups could reduce the concentration of ammonia nitrogen to less than 10 mg/L within 48 h, and there was no significant accumulation of nitrate nitrogen and nitrite nitrogen during the whole reaction process. The accumulation of nitrate and nitrite nitrogen was not obvious during the whole reaction. The pH of each group in the system increased slightly from 0 to 12 h and then decreased continuously. The pH of the 1:1 and 2:1 groups increased continuously after 48 h, and the pH of the other three groups increased slightly after 60 h. The final pH values of each group from low to high by mass ratio were 6.33, 5.34, 4.84, 4.64 and 4.55, respectively.

The NH_4^+-N removal efficiency of BC400 + BC700 + Z03 system and the control group at 72h are shown in Fig. 5b.The results indicated that the NH_4^+-N removal efficiency by BC400 + BC700 system at 72h is lower than 10% when the dosage is 3.0g/L, while the removal rate of ammonia nitrogen after coupling Z03 is all located between 93.58% and 95.05%, which is much higher than that of only adding biochar or only strain Z03. At 72 h, the pH of all groups in the BC400 + BC700 system was between 7.5 ± 0.4, and the pH of all

groups in the BC400 + BC700 + Z03 system gradually decreased from 6.5 to 4.5 with the increase of the BC400:BC700 mass ratio.

Figure 5 Variation of NH_4^+-N concentration, pH, NO_3^--N and NO_2^--N concentration in BC400 + BC700 + Z03 system with different biochar mass ratio (a); comparison of 72h NH_4^+-N removal efficiency and pH change between BC400 + BC700 + Z03 system and control group with different biochar mass ratio (b).

Environment pH affects the adsorption performance of biochar and the growth and metabolic capacity of microorganisms. To investigate the effect of initial pH on different NH_4^+-N removal systems, the NH_4^+-N removal efficiency of each system at different initial pH was observed when BC400 and BC700 were dosed at 3.0 g/L with a mass ratio of 5:1. The change of NH_4^+-N concentration, pH, NO_3^--N and NO_2^--N concentration in 72 h are shown in Fig. 6a. It indicated that the NH_4^+-N concentration in all groups continued to decrease to below 5 mg/L within 72 h. The higher the starting pH, the faster the NH_4^+-N concentration decreased, and NO_3^--N and NO_2^--N overall fluctuated in the lower concentration range without significant accumulation. The pH of each group continued to decrease within 48 h of the reaction, and after 48 h the pH of the groups with starting pH of 7.5, 8.5 and 9.5 slightly recovered, while the pH of the remaining groups continued to decrease, and the final pH of each group was 7.63, 7.31, 6.6, 5.19, 4.51 and 4.47, respectively, according to the starting pH from high to low.

The results of NH_4^+-N removal efficiency of BC400 + BC700 + Z03 system and control group at different initial pH at 72 h are shown in Fig. 6b. The figure demonstrated that the NH_4^+-N removal efficiency of each group with biochar only increased with the increase of initial pH, and the highest NH_4^+-N removal efficiency of 31.23% was achieved at the initial pH of 10.5, while the NH_4^+-N removal efficiency of the rest of the groups was lower than 20% within 72 h. The NH_4^+-N removal efficiency in the groups inoculated with strain Z03 only were in the range of 30 ~ 43%, and the alkaline environment had a certain inhibitory effect on microbial HNAD process under the low C/N ratio. All groups of the mixed biochar coupled with strain Z03 nitrogen removal system could achieve more than 95% NH_4^+-N removal efficiency at 72 h,and the removal rate increased slightly with the increase of the initial pH.

BC400 and BC700, as materials with good redox activity, may play a role in promoting electron transfer system activity and enzyme activity during biological denitrification. Previous studies (Klüpfel et al., 2014; X. Xu et al., 2019)have shown that, the low-temperature biochar has a better electron supply capacity than the high-temperature biochar, and the high-temperature biochar has the role of an electron shuttle mediator that can facilitate electron transfer, and this result is consistent with the FTIR analysis of BC400 and BC700. Wu et al. (Wu et al., 2019b) showed that biochar at 300°C significantly enhanced the activity of the electron transfer system of denitrifying microorganisms and promoted their utilization rate of carbon sources, and in addition, compared to high-temperature biochar, low-temperature biochar increased the activity of denitrifying enzymes NAR and NIR, which in turn increased the denitrification rate. Thus, it is speculated that the high dosage of BC400 + Z03 NH_4^+-N removal efficiency is slightly

better than BC700 + Z03 in the denitrification reaction because BC400 is more effective in promoting the activity of nitrilase and denitrifying enzymes, while the significant increase in the reaction rate of BC400 + BC700 + Z03 compared with the previous two may be due to the electron transfer capacity of BC700 which promotes the ability of BC400 as an electron donor to increase the activity of the reaction electron transfer system. The significant increase in the reaction rate of BC400 + BC700 + Z03 system compared to BC400/BC700 + Z03 system may be due to the ability of BC400 as an electron donor to enhance the activity of the reaction electron transfer system. However, the difference in the NH_4^+-N removal efficiency of these three systems was significantly smaller than that of 48 h after 72 h. Therefore, it was speculated that the mixed biochar system could improve the reaction rate by enhancing the activity of the electron transfer system, and the final NH_4^+-N removal effect was mainly influenced by the content of DOC contained in the biochar and the pH retarding effect.

Figure 6 Variation of NH_4^+-N concentration, pH, NO_3^--N and NO_2^--N concentration in BC400 + BC700 + Z03 system with different initial pH (a); comparison of 72h NH_4^+-N removal efficiency and pH change between BC400 + BC700 + Z03 system and control group with different initial pH (b).

4. Conclusion

The biochar BC400 and BC700 were prepared by the oxygen-limited temperature control method, and characterized by SEM, BET, FITR, XRD, RS, DOC, zeta potential and elemental analysis. It was found that with the increase of carbonization temperature, BC700 had higher specific surface area and more multilayer pore size structure, increased aromatic condensation, higher crystallinity and more ordered structure. Both of them have better redox activity, BC400 has stronger electron donor ability and BC700 has better electron transfer performance. BC400 and BC700 contained relatively high DOC contents of 62.95 and 51.617 mg/g, respectively. BC400/BC700 + Z03 system was able to significantly improve the NH_4^+-N removal effect on low temperature low C/N containing wastewater compared to the control group (biochar only/ strain Z03 only i). The BC400 + BC700 + Z03 system has a faster NH_4^+-N removal rate compared to the BC400/BC700 + Z03 system. The promotion of strain Z03 by biochar may be due to the ability of biochar to provide a carbon source for strain Z03, to achieve pH retardation and to promote the activity of electron transfer systems and enzymes in HNAD process.

Declarations

Ethics approval and consent to participate. Not applicable.

Consent for publication. Not applicable.

Availability of data and material. All data generated or analysed during this study are included in this published article [and its supplementary information files].

Competing interests. There are no conflicts of interest to declare.

Funding. This work was supported by the National Natural Science Foundation of China [grant numbers31700433, 31672314].

Authors' contributions. M.T. and J.J. conceived the idea and designed the experiments. J.J. and X.X. conducted experiments. J.J. analyzed data and wrote the paper. All authors discussed the results and commented on the manuscript.

Acknowledgement. The authors gratefully thank the financial support provided by the National Natural Science Foundation of China (No. 31700433; No. 31672314).

Conflicts of interest

The authors declare that there are no conflicts of interest regarding the publication of this article.

References

Ahmad, M., Rajapaksha, A.U., Lim, J.E., Zhang, M., Bolan, N., Mohan, D., Vithanage, M., Lee, S.S., Ok, Y.S., 2014a. Biochar as a sorbent for contaminant management in soil and water: A review. Chemosphere 99, 19–33. https://doi.org/10.1016/j.chemosphere.2013.10.071

Ahmad, M., Rajapaksha, A.U., Lim, J.E., Zhang, M., Bolan, N., Mohan, D., Vithanage, M., Lee, S.S., Ok, Y.S., 2014b. Biochar as a sorbent for contaminant management in soil and water: A review. Chemosphere 99, 19–33. https://doi.org/10.1016/j.chemosphere.2013.10.071

Chen, S., He, S., Wu, C., Du, D., 2019. Characteristics of heterotrophic nitrification and aerobic denitrification bacterium Acinetobacter sp. T1 and its application for pig farm wastewater treatment. J. Biosci. Bioeng. 127, 201–205. https://doi.org/10.1016/j.jbiosc.2018.07.025

Chen, Y., Yu, B., Lin, J., Naidu, R., Chen, Z., 2016. Simultaneous adsorption and biodegradation (SAB) of diesel oil using immobilized Acinetobacter venetianus on porous material. Chem. Eng. J. 289, 463–470. https://doi.org/10.1016/j.cej.2016.01.010

Feng, B., Bhatia, S.K., Barry, J.C., 2002. Structural ordering of coal char during heat treatment and its impact on reactivity. Carbon N. Y. 40, 481–496. https://doi.org/10.1016/S0008-6223(01)00137-3

Galloway, J.N., Townsend, A.R., Erisman, J.W., Bekunda, M., Cai, Z., Freney, J.R., Martinelli, L.A., Seitzinger, S.P., Sutton, M.A., 2008. Transformation of the nitrogen cycle: Recent trends, questions, and potential solutions. Science (80-.). 320, 889–892. https://doi.org/10.1126/science.1136674

Gao, Q.T., Wong, Y.S., Tam, N.F.Y., 2011. Removal and biodegradation of nonylphenol by immobilized Chlorella vulgaris. Bioresour. Technol. 102, 10230–10238. https://doi.org/10.1016/j.biortech.2011.08.070

Guerrero, M., Ruiz, M.P., Millera, Á., Alzueta, M.U., Bilbao, R., 2008. Characterization of biomass chars formed under different devolatilization conditions: Differences between rice husk and Eucalyptus. Energy

and Fuels 22, 1275–1284. https://doi.org/10.1021/ef7005589

Huang, W., Zhang, B., Feng, C., Li, M., Zhang, J., 2012. Research trends on nitrate removal: a bibliometric analysis. Desalin. Water Treat. 50, 67–77. https://doi.org/10.1080/19443994.2012.708542

Jie, Z.H.U., He-, C., 2018. Analysis of Current Situation and Potential Evaluation of Upgrading and Reconstruction of Municipal Wastewater Treatment Plant in Shanghai. https://doi.org/10.19853/j.zgjsps.1000-4602.2018.12.004

Klüpfel, L., Keiluweit, M., Kleber, M., Sander, M., 2014. Redox properties of plant biomass-derived black carbon (biochar). Environ. Sci. Technol. 48, 5601–5611. https://doi.org/10.1021/es500906d

Li, C., Yang, J., Wang, X., Wang, E., Li, B., He, R., Yuan, H., 2015. Removal of nitrogen by heterotrophic nitrification-aerobic denitrification of a phosphate accumulating bacterium Pseudomonas stutzeri YG-24. Bioresour. Technol. 182, 18–25. https://doi.org/10.1016/j.biortech.2015.01.100

Li, H., Li, Y., Xu, Y., Lu, X., 2020. Biochar phosphorus fertilizer effects on soil phosphorus availability. Chemosphere 244. https://doi.org/10.1016/j.chemosphere.2019.125471

Liu, C.H., Chu, W., Li, H., Boyd, S.A., Teppen, B.J., Mao, J., Lehmann, J., Zhang, W., 2019. Quantification and characterization of dissolved organic carbon from biochars. Geoderma 335, 161–169. https://doi.org/10.1016/j.geoderma.2018.08.019

Liu, Y., Wang, J., 2019. Reduction of nitrate by zero valent iron (ZVI)-based materials: A review. Sci. Total Environ. 671, 388–403. https://doi.org/10.1016/j.scitotenv.2019.03.317

Lou, L., Huang, Q., Lou, Y., Lu, J., Hu, B., Lin, Q., 2019. Adsorption and degradation in the removal of nonylphenol from water by cells immobilized on biochar. Chemosphere 228, 676–684. https://doi.org/10.1016/j.chemosphere.2019.04.151

Marsh, H., 1987. Adsorption methods to study microporosity in coals and carbons-a critique. Carbon N. Y. 25, 49–58. https://doi.org/10.1016/0008-6223(87)90039-X

Mukherjee, A., Zimmerman, A.R., 2013. Organic carbon and nutrient release from a range of laboratory-produced biochars and biochar-soil mixtures. Geoderma 193–194, 122–130. https://doi.org/10.1016/j.geoderma.2012.10.002

Ren, Y.X., Yang, L., Liang, X., 2014. The characteristics of a novel hfile:///Users/zzj/Desktop/CESE/□□□□□/□□□44.pdfeterotrophic nitrifying and aerobic denitrifying bacterium, Acinetobacter junii YB. Bioresour. Technol. 171, 1–9. https://doi.org/10.1016/j.biortech.2014.08.058

Sima, X.F., Li, B.B., Jiang, H., 2017. Influence of Pyrolytic Biochar on Settleability and Denitrification of Activated Sludge Process. Chinese J. Chem. Phys. 30, 357–364. https://doi.org/10.1063/1674-0068/30/cjcp1612230

Steinbeiss, S., Gleixner, G., Antonietti, M., 2009. Effect of biochar amendment on soil carbon balance and soil microbial activity. Soil Biol. Biochem. 41, 1301–1310. https://doi.org/10.1016/j.soilbio.2009.03.016

Tang, J., Li, X., Luo, Y., Li, G., Khan, S., 2016. Spectroscopic characterization of dissolved organic matter derived from different biochars and their polycylic aromatic hydrocarbons (PAHs) binding affinity. Chemosphere 152, 399–406. https://doi.org/10.1016/j.chemosphere.2016.03.016

Tang, M., Jiang, J., Lv, Q., Yang, B., Zheng, M., Gao, X., Han, J., Zhang, Y., Yang, Y., 2020. Denitrification performance of Pseudomonas fluorescens Z03 immobilized by graphene oxide-modified polyvinyl-alcohol and sodium alginate gel beads at low temperature. R. Soc. Open Sci. 7. https://doi.org/10.1098/rsos.191542

Wang, B., Qiu, J., Feng, H., Sakai, E., Komiyama, T., 2016. KOH-activated nitrogen doped porous carbon nanowires with superior performance in supercapacitors. Electrochim. Acta 190, 229–239. https://doi.org/10.1016/j.electacta.2016.01.038

Wang, C., Xu, Y., Hou, J., Wang, P., Zhang, F., Zhou, Q., You, G., 2019. Zero valent iron supported biological denitrification for farmland drainage treatments with low organic carbon: Performance and potential mechanisms. Sci. Total Environ. 689, 1044–1053. https://doi.org/10.1016/j.scitotenv.2019.06.488

Wang, S., Zhao, M., Zhou, M., Li, Y.C., Wang, J., Gao, B., Sato, S., Feng, K., Yin, W., Igalavithana, A.D., Oleszczuk, P., Wang, X., Ok, Y.S., 2019. Biochar-supported nZVI (nZVI/BC) for contaminant removal from soil and water: A critical review. J. Hazard. Mater. 373, 820–834. https://doi.org/10.1016/j.jhazmat.2019.03.080

Wu, Z., Xu, F., Yang, C., Su, X., Guo, F., Xu, Q., Peng, G., He, Q., Chen, Y., 2019a. Highly efficient nitrate removal in a heterotrophic denitrification system amended with redox-active biochar: A molecular and electrochemical mechanism. Bioresour. Technol. 275, 297–306. https://doi.org/10.1016/j.biortech.2018.12.058

Wu, Z., Xu, F., Yang, C., Su, X., Guo, F., Xu, Q., Peng, G., He, Q., Chen, Y., 2019b. Highly efficient nitrate removal in a heterotrophic denitrification system amended with redox-active biochar: A molecular and electrochemical mechanism. Bioresour. Technol. 275, 297–306. https://doi.org/10.1016/j.biortech.2018.12.058

Xu, X., Huang, H., Zhang, Y., Xu, Z., Cao, X., 2019. Biochar as both electron donor and electron shuttle for the reduction transformation of Cr(VI) during its sorption. Environ. Pollut. 244, 423–430. https://doi.org/10.1016/j.envpol.2018.10.068

Xu, Z., Xu, X., Tao, X., Yao, C., Tsang, D.C.W., Cao, X., 2019. Interaction with low molecular weight organic acids a ff ects the electron shuttling of biochar for Cr (VI) reduction. J. Hazard. Mater. 378, 120705. https://doi.org/10.1016/j.jhazmat.2019.05.098

Yang, Y.W., Duan, X.Y., Jiang, J., Xu, X.Y., Tang, M.Z., 2020. Immobilization of cold-resistant mixed bacteria and its application in sequencing batch reactor wastewater treatment. Appl. Ecol. Environ. Res. 18, 515–529. https://doi.org/10.15666/aeer/1801_515529

Yu, C.Q., Huang, X., Chen, H., Godfray, H.C.J., Wright, J.S., Hall, J.W., Gong, P., Ni, S.Q., Qiao, S.C., Huang, G.R., Xiao, Y.C., Zhang, J., Feng, Z., Ju, X.T., Ciais, P., Stenseth, N.C., Hessen, D.O., Sun, Z.L., Yu, L., Cai, W.J., Fu, H.H., Huang, X.M., Zhang, C., Liu, H. Bin, Taylor, J., 2019. Managing nitrogen to restore water quality in China. Nature 567, 516–520. https://doi.org/10.1038/s41586-019-1001-1

Yu, Y., Wan, Y., Shang, H., Wang, B., Zhang, P., Feng, Y., 2019. Corncob-to-xylose residue (CCXR) derived porous biochar as an excellent adsorbent to remove organic dyes from wastewater. Surf. Interface Anal. 51, 234–245. https://doi.org/10.1002/sia.6575

Yuan, J.H., Xu, R.K., Zhang, H., 2011. The forms of alkalis in the biochar produced from crop residues at different temperatures. Bioresour. Technol. 102, 3488–3497. https://doi.org/10.1016/j.biortech.2010.11.018

Zhang, Q.L., Liu, Y., Ai, G.M., Miao, L.L., Zheng, H.Y., Liu, Z.P., 2012. The characteristics of a novel heterotrophic nitrification-aerobic denitrification bacterium, Bacillus methylotrophicus strain L7. Bioresour. Technol. 108, 35–44. https://doi.org/10.1016/j.biortech.2011.12.139

Zhang, X., Davidson, E.A., Mauzerall, D.L., Searchinger, T.D., Dumas, P., Shen, Y., 2015. Managing nitrogen for sustainable development. Nature 528, 51–59. https://doi.org/10.1038/nature15743

Figures

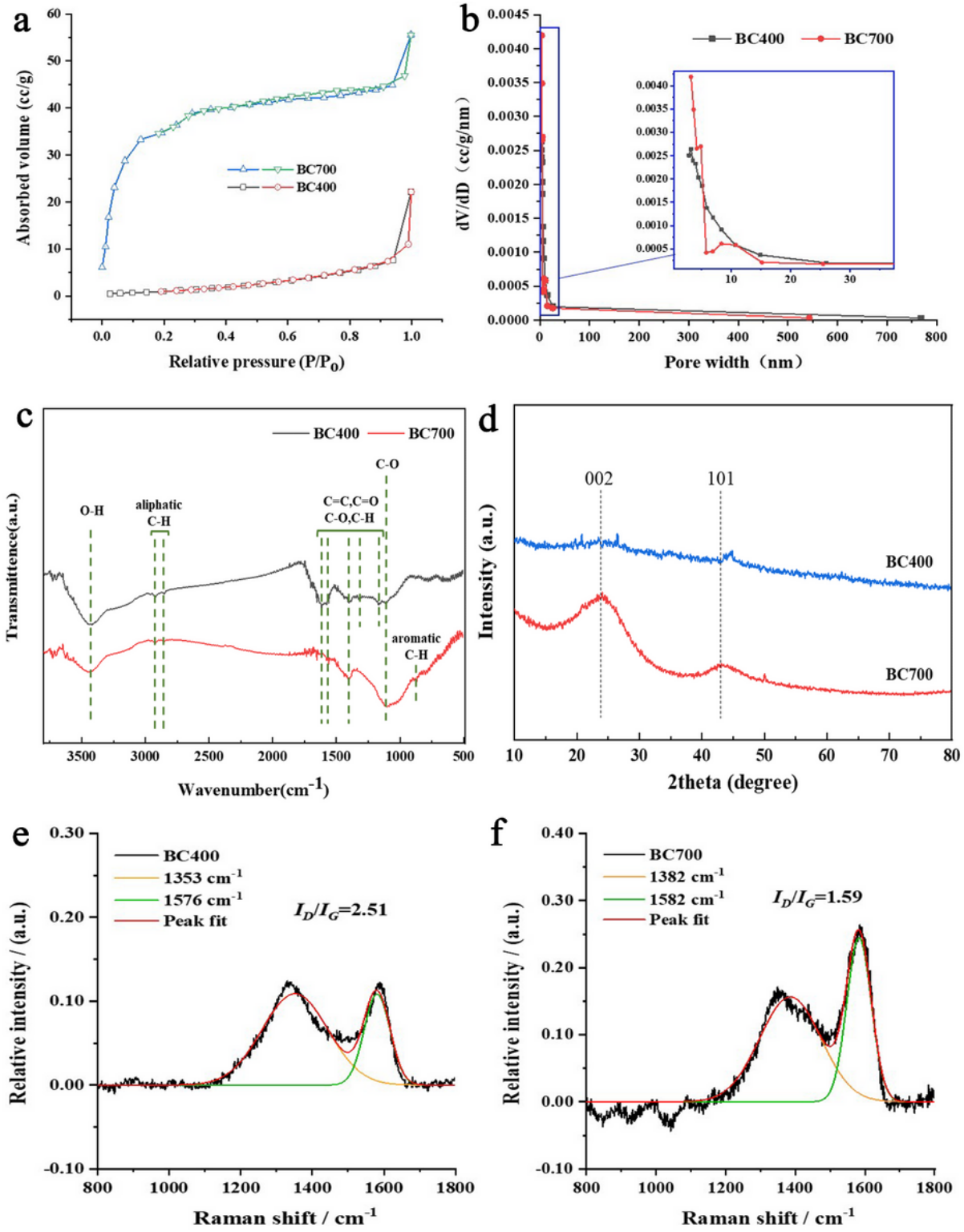

Figure 1

Nitrogen adsorption-desorption isotherms of BC400 and BC700 (a); pore size distribution of BC400 and BC700(b); FTIR spectrograms of BC400 and BC700(c); XRD spectrograms of BC400 and BC700 (d); Raman spectrograms of BC400 (e) and BC700 (f).

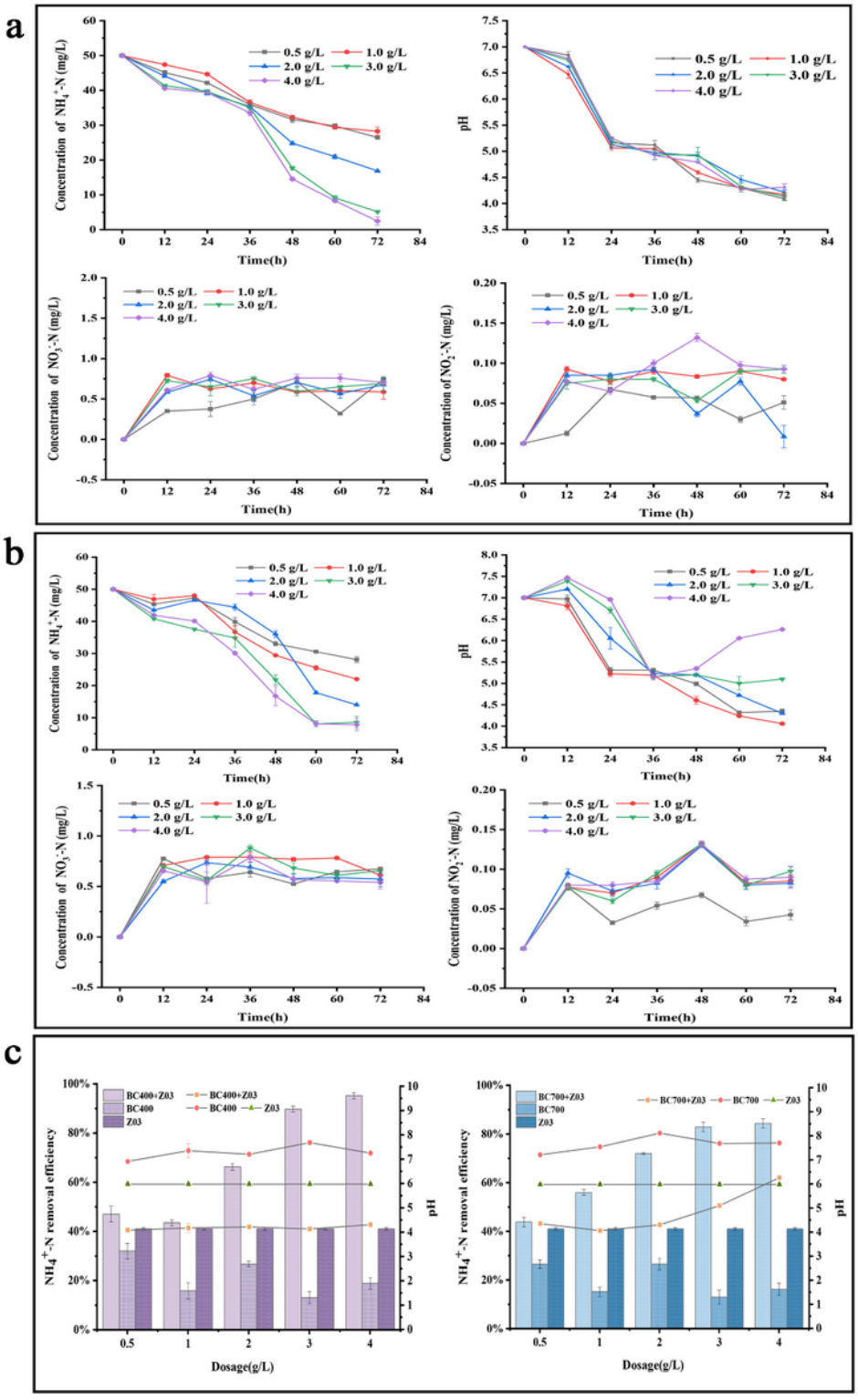

Figure 2

Variation of NH4+-N concentration, pH, NO3–N and NO2–N concentration in BC400+Z03 (a) and BC700+Z03 (b) systems with different dosages; comparison of NH4+-N removal efficiency and pH between BC400/BC700+Z03 systems and control group at different dosages for 72h (c).

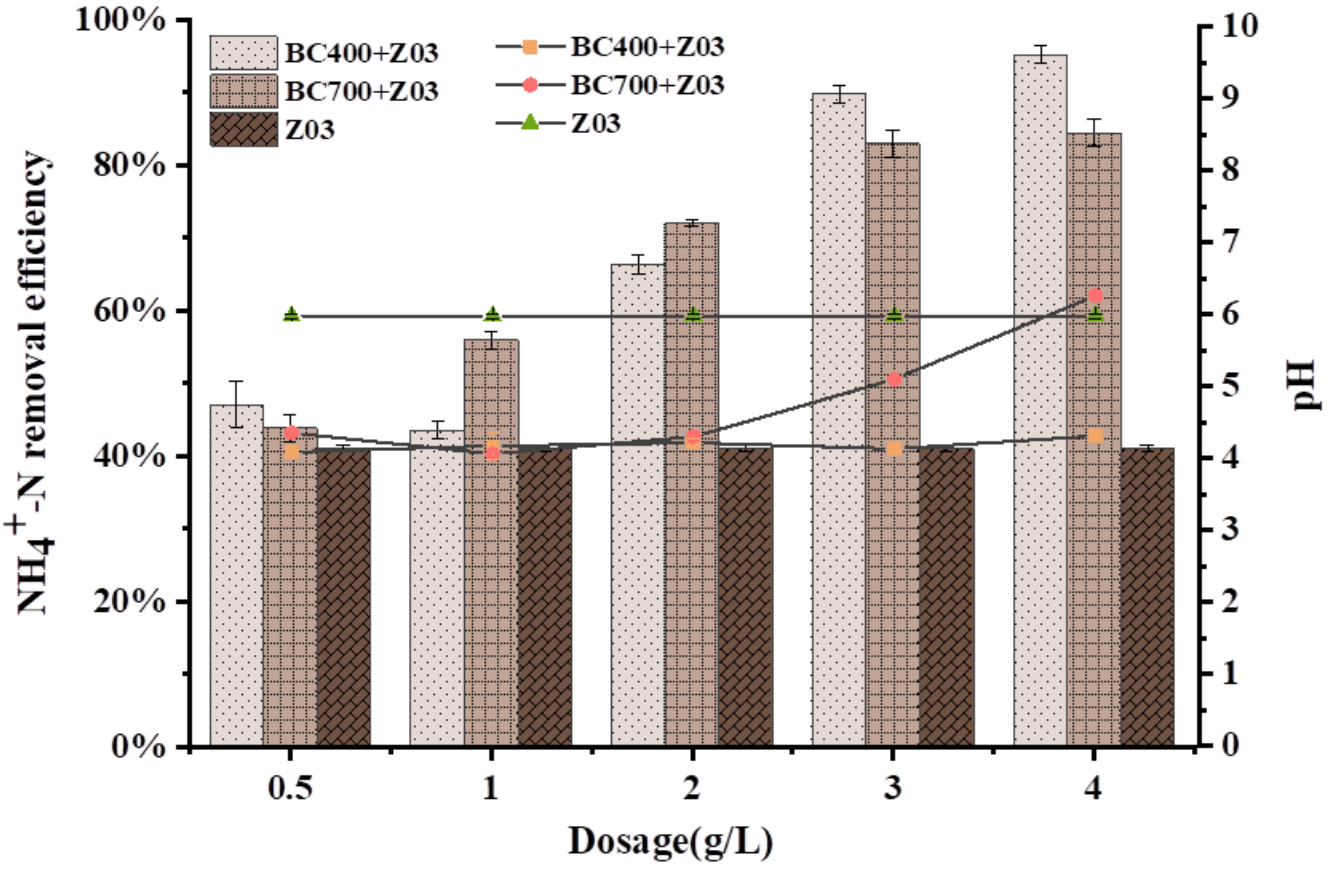

Figure 3

Comparison of 72h NH4+-N removal rate and pH change between BC400/BC700+Z03 and strain Z03 systems with different biochar dosages

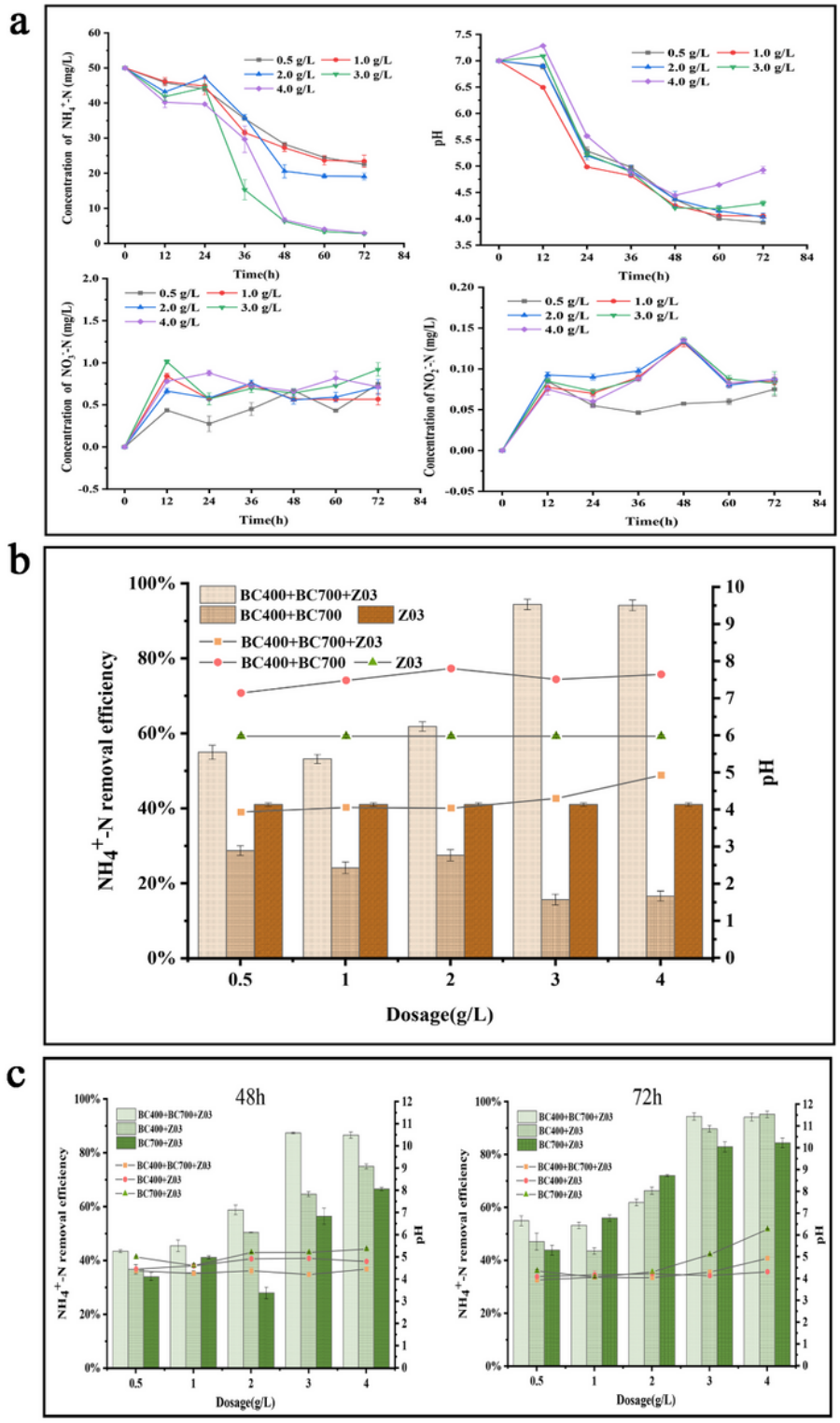

Figure 4

Variation of NH4+-N concentration, pH, NO3--N and NO2--N concentration in BC400+BC700+Z03 system with different biochar dosages (a); comparison of NH4+-N removal efficiency and pH between BC400+BC700+Z03 systems and control group at different biochar dosages for 72h (b); comparison of NH4+-N removal efficiency and pH between BC400+BC700+Z03 and BC400 BC400/BC700+Z03 systems with different biochar dosages(c).

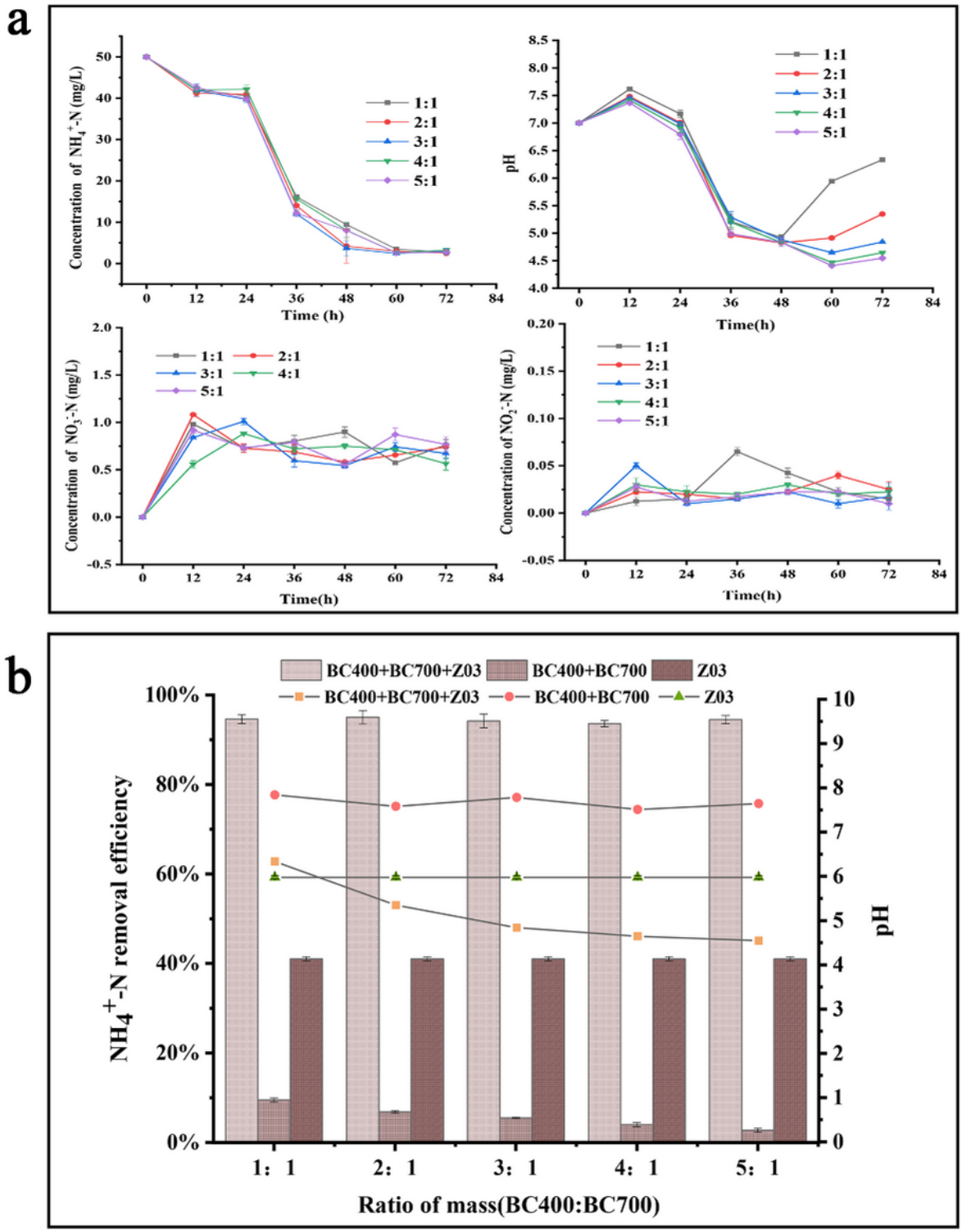

Figure 5

Variation of NH4+-N concentration, pH, NO3–N and NO2–N concentration in BC400+BC700+Z03 system with different biochar mass ratio (a); comparison of 72h NH4+-N removal efficiency and pH change between BC400+BC700+Z03 system and control group with different biochar mass ratio (b).

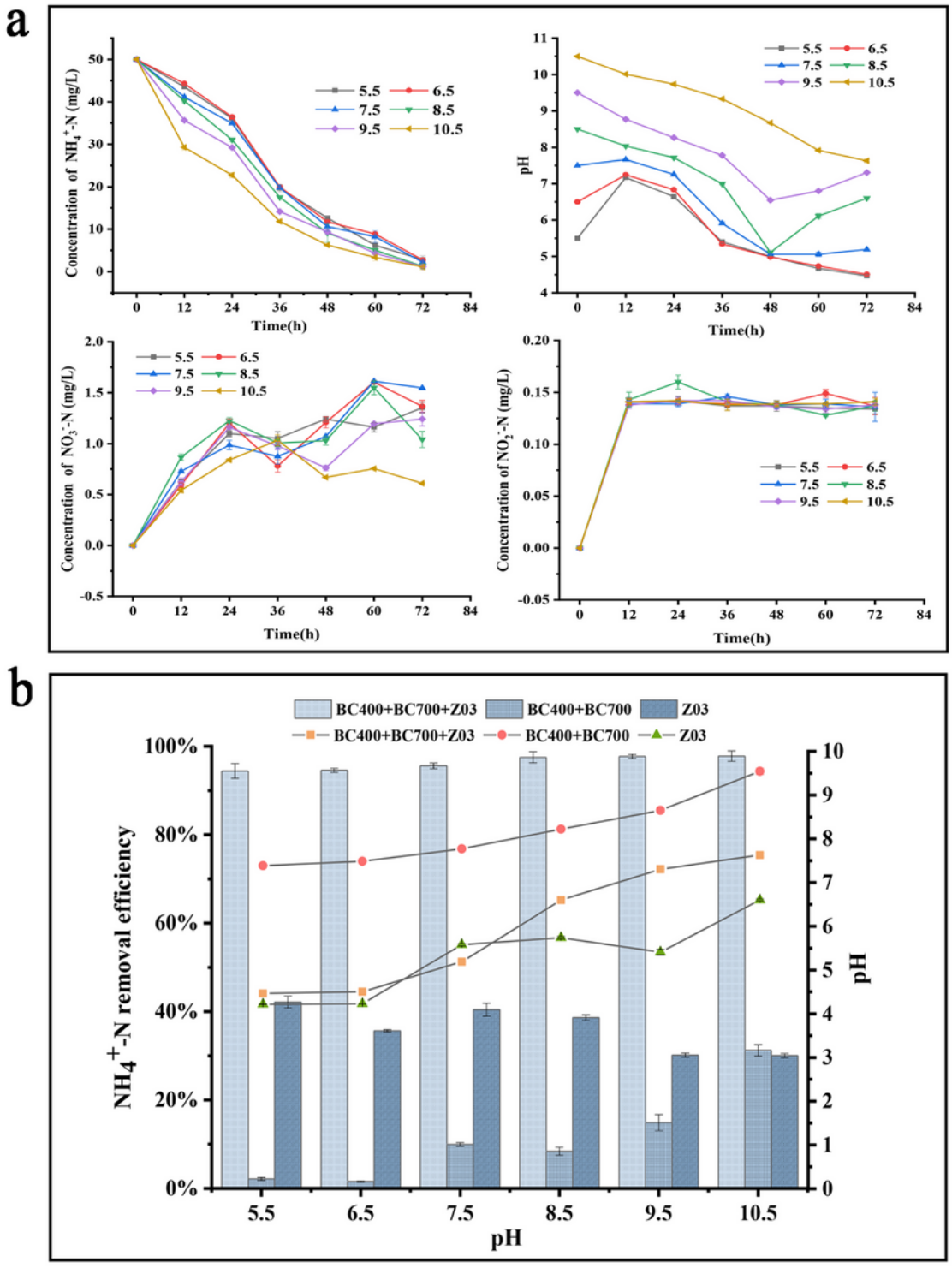

Figure 6

Variation of NH4+-N concentration, pH, NO3–N and NO2–N concentration in BC400+BC700+Z03 system with different initial pH (a); comparison of 72h NH4+-N removal efficiency and pH change between BC400+BC700+Z03 system and control group with different initial pH (b).

Supplementary Files

This is a list of supplementary files associated with this preprint. Click to download.

- SI.docx